Research Article

Magnetic Resonance in Chemistry

Received: 13 December 2007 Revised: 10 January 2008 Accepted: 14 January 2008 Published online in Wiley Interscience: 28 March 2008

(www.interscience.com) DOI 10.1002/mrc.2201

Characterization of nonderivatized plant cell walls using high-resolution solution-state NMR spectroscopy†

Daniel J. Yelle,[a,b]* John Ralph[c,d] and Charles R. Frihart[a]

A recently described plant cell wall dissolution system has been modified to use perdeuterated solvents to allow direct in-NMR-tube dissolution and high-resolution solution-state NMR of the whole cell wall without derivatization. Finely ground cell wall material dissolves in a solvent system containing dimethylsulfoxide-d_6 and 1-methylimidazole-d_6 in a ratio of 4 : 1 (v/v), keeping wood component structures mainly intact in their near-native state. Two-dimensional NMR experiments, using gradient-HSQC (heteronuclear single quantum coherence) 1-bond $^{13}C-^{1}H$ correlation spectroscopy, on nonderivatized cell wall material from a representative gymnosperm *Pinus taeda* (loblolly pine), an angiosperm *Populus tremuloides* (quaking aspen), and a herbaceous plant *Hibiscus cannabinus* (kenaf) demonstrate the efficacy of the system. We describe a method to synthesize 1-methylimidazole-d_6 with a high degree of perdeuteration, thus allowing cell wall dissolution and NMR characterization of nonderivatized plant cell wall structures. **Copyright © 2008 John Wiley & Sons, Ltd.**

Supplementary electronic material for this paper is available in Wiley InterScience at http://www.interscience.wiley.com/jpages/0749-1581/suppmat/

Keywords: NMR; HSQC; 1-methylimidazole-d_6; dimethylsulfoxide-d_6; *Pinus taeda*; *Populus tremuloides*; *Hibiscus cannabinus*; whole cell wall dissolution; lignin; polysaccharides

Introduction

Characterizing plant cell wall composition and structure requires a variety of approaches. Nondestructive spectroscopic methods that can be applied to the cell wall (or whole plant material), including solid-state NMR, IR, NIR, are often limited because of either poor resolution and/or poor structural determination. Degradative methods may be applied to the whole cell wall material, but study of individual components typically requires their separation. Improved solid-state NMR has been useful for examining the intact plant cell walls[1–4]; however, the decreased relaxation times and low peak dispersion with solid-state NMR limit its use for thorough characterization of intact polymers. As solution-state NMR instrumentation and experiments become more developed, higher sensitivity and resolution permit the detailed structural analysis of cell wall polymeric components more effectively. Recently, two solvent systems were developed for cell wall dissolution to allow quite detailed structural analysis of the entire cell wall (following ball-milling), without component separation or degradation via high-resolution solution-state NMR.[5] These methods inspired the logical modification of one of these solvent systems to characterize the cell wall following dissolution, i.e. without derivatization or work-up steps.

Secondary xylem is the anatomical tissue distinguishing a woody plant from a nonwoody plant. It is the xylem cells, tracheids (gymnosperms) and libriform fibers and vessels (angiosperms) that house the genetic capability to biosynthesize lignified woody cells. On a microscale, the cell wall consists of a middle lamella, primary wall, and three secondary wall layers (S1, S2, and S3), where S2 is the most substantial. After the cell wall polysaccharides (cellulose and various hemicelluloses) are synthesized and assembled, *p*-hydroxycinnamyl alcohols are exported to the wall and are polymerized through radical coupling mechanisms to form a polymeric matrix (lignin), in which the polysaccharides are embedded. Thus, it is the lignin that acts as the mortar to support the polysaccharides. The plant cell wall, therefore, may be regarded as a highly complex nanocomposite.

Component isolation remains a valuable method to obtain relatively pure fractions of individual wall polymers or polymer classes. Isolating lignin, cellulose, and hemicelluloses from wood has been long known to be a difficult task, since none of these components can be removed without either significant chemical or mechanical modification of the cell wall. Many attempts have been made to mill the cell wall to extract lignin and polysaccharides. Björkman[6] in 1956 was one of the first to isolate up to 50% of a 'native' lignin from ball-milled spruce via extraction with aqueous dioxane to give what is called milled-wood lignin. The carbohydrate-free yield in practice is usually less than 30% of the total lignin, and is highly dependent on milling efficiency and the type of plant. Treating ball-milled plant cell walls with a cellulolytic enzyme that served to hydrolyze the polysaccharides allowed the isolation of a cellulolytic enzyme lignin,[7] which retained

* *Correspondence to: Daniel J. Yelle, USDA Forest Service, Forest Products Laboratory, One Gifford Pinchot Dr., Madison, WI 53726, USA. E-mail: dyelle@fs.fed.us*

a *USDA Forest Service, Forest Products Laboratory, Madison, Wisconsin, USA*

b *Department of Forestry, University of Wisconsin-Madison, USA*

c *US Dairy Forage Research Center, Madison, Wisconsin, USA*

d *Department of Biological Systems Engineering, University of Wisconsin, USA*

† *This article was published online on 28 March 2008. An error was subsequently identified and corrected by an erratum notice that was published online only on 23 April 2008; DOI: 10.1002/mrc.2251. This printed version incorporates the amendment identified in the erratum notice.*

Copyright © 2008 John Wiley & Sons, Ltd.

essentially all the lignin, but also a substantial fraction of the polysaccharides.

Isolation of polysaccharide components from plant cell walls typically involves the removal of lignin to obtain a holocellulose. Maple holocellulose has been isolated with chlorination and extraction of the lignin with 15% pyridine in ethanol.[8] Sodium chlorite in acid solution on cell wall material retains hemicelluloses almost quantitatively.[9–11] Complete delignification, without significant loss of polysaccharides, is not obtainable by these methods. Isolation of specific hemicelluloses in the cell wall must be gently extracted and purified so as to maintain as natural a state as possible. A neutral solvent, such as dimethylsulfoxide (DMSO), is useful for extracting holocellulose to obtain a xylan fraction with little structural change. Alkaline (KOH or NaOH) solutions containing sodium borate allow extraction of galactoglucomannans and glucomannans. However, alkali facilitates deacetylaton of xylans and mannans. Pretreatments, such as steam exposure (with and without explosion), on aspen or birch for 10 min and subsequent water extraction, yields mainly acetyl substituted xylans.[12] To extract the naturally acetylated mannans, thermomechanical pulp of spruce (2% consistency) may be suspended in distilled water with stirring at 60 °C,[13] while spruce holocellulose may be extracted with boiling water to obtain the same.[14] Further isolation of holocellulose components involves alkaline extraction, but the remaining α-cellulose steadfastly retains some mannan and xylan.

Methods that involve ball-milling are the basis of several cell wall characterization procedures, but ball-milling itself breaks bonds and therefore causes structural changes. Knowing the effect that ball-milling has on plant cell walls is important because milling the cell wall destroys anatomical information that once existed. It has been found that the intensity (ball-mill frequency) of milling has a larger influence on the particle size than prolonging of the milling time and that the cell corners and middle lamella are the most resistant layers to milling, whereas the S1 and S2 layers are clearly fibrillated early in the milling process.[15,16] These studies suggest that most, if not all, of the extractable cell wall components are obtained from these secondary cell wall layers, and not from the whole cell wall.

Nondestructively dissolving plant cell walls to better understand its native chemical structure has been a challenge. Many investigators examined solvent systems that dissolve cellulose (e.g. dimethylacetamide/LiCl), because this highly crystalline component was anticipated to be the most difficult to dissolve. With the introduction of newer ionic liquids, compounds such as 1-*N*-butyl-3-methylimidazolium chloride[17] and 1-allyl-3-methylimidazolium chloride[18] have been introduced for cellulose dissolution at temperatures >80 °C. The underlying benefits of these solvents are the ease of recycling them because of their low vapor pressure. However, for the purposes of dissolving the plant cell wall, dissolution temperatures beyond 50 °C begin to approach the thermal transition points of lignin, thus increasing the probability of degradation. Specific ionic liquids do have the capability of dissolving plant cell wall material,[19–21] but the lack of degradative assessments of these systems currently limit their application in structural studies. Two systems that were shown to be effective and nondegradative in dissolving ball-milled plant cell walls have been recently described.[5] DMSO with tetrabutylammonium fluoride (TBAF),[22] or DMSO with 1-methylimidazole (or *N*-methylimidazole, NMI) fully dissolves plant cell walls at room temperature. It is currently not well understood how these solvents act to facilitate dissolution. We hypothesize that NMI has the capability of disrupting the strong hydrogen bonding interactions between cellulose and other components to allow DMSO (a good swelling solvent for woody plants) further access to the cell wall structure. *In situ* acetylation may be performed to a high degree of substitution so that the resulting acetylated cell wall material dissolves in $CDCl_3$ for NMR experiments. The cellulose, albeit after the degree of polymerization is dramatically decreased by ball-milling, from the DMSO/NMI system appears to remain intact. This nondegradative dissolution (followed by acetylation) allows characterization of the ball-milled whole cell wall to a much higher resolution than is possible with solid-state NMR.

To learn more about the reactivity or degradation of various cell wall components, we needed to find a way to dissolve the whole cell wall, without derivatization, in suitable NMR solvents. Again, if the whole cell wall is dissolved in a less modified state, chemical interactions with various components may be characterized via solution-state NMR. The DMSO/NMI system will fully dissolve the whole cell wall. Logically, then, utilizing both perdeuterated DMSO and NMI should allow direct NMR analysis of nonderivatized walls, without the influence of strong solvent resonances. Characterizing the chemistry of the nonderivatized plant cell wall via gradient heteronuclear single quantum coherence (HSQC) 1-bond $^{13}C-^{1}H$ correlations depicts the plant cell wall polymers in a fairly native state and, although it is well recognized that ball-milling already causes significant depolymerization of cell wall polymers; an advantage is that the native polymeric structures that are often obscured by traditional derivatization or isolation practices can be studied. For example, natural acetates, found on syringyl units of lignin, especially in kenaf bast fibers, are known to acylate a substantial fraction of the side chains of lignin units (primarily at the γ position)[23–25] and are masked in NMR spectra by the current practice of acetylating the cell wall. Also, hemicelluloses like galactoglucomannan and glucuronoxylan contain acetyl side groups off their main chain, which should be fully distinguishable by NMR.

Our approach is to leave the plant cell wall material in a minimally altered state so as to characterize all components without requiring extensive component extraction or isolation techniques. By doing so, we leave the cell wall component polymers essentially unchanged, thus enabling the characterization of specific cell wall structures not seen before through NMR.

In this paper, we describe the following: (i) synthesis of perdeuterated NMI, (ii) dissolution of the plant cell wall in the most minimally altered state currently possible, and (iii) determination of chemical shifts of various polymeric plant cell wall structures via solution-state NMR techniques. The use of these techniques enables the characterization of specific cell wall components that may be partially reacted during derivatization or biological degradation, and allows the approximate quantification of natural acetates found in lignin and hemicelluloses.

Experimental

Chemicals

Ruthenium (III) chloride hydrate (35–40% Ru), tributyl phosphite (94%), and methanol-d_4 (99.8% D) were supplied by Acros Organics (Geel, Belgium). Imidazole (recrystallized), 1,4-dioxane (98%), palladium on activated carbon (10% Pd), D_2O (99.9% D), chloroform-d (99.8% D), and dimethylsulfoxide-d_6 (99.5% D) were supplied by Aldrich Chemical Company (Milwaukee, WI).

Copyright © 2008 John Wiley & Sons, Ltd.

Synthesis of 1-methyl-d_3-imidazole

This synthesis is derived from prior published syntheses.[26,27] Briefly, imidazole (10.89 g, 160 mmol), tributylphosphite (2.30 g, 9.2 mmol), ruthenium chloride hydrate (0.64 g, 3.1 mmol), and methanol-d_4 (20 g, 555 mmol) were sequentially added to dioxane (300 ml) in a 2-l stainless steel Parr reactor vessel. The vessel was sequentially sealed, purged with nitrogen, stirred, heated to 200 °C, and pressurized with nitrogen to 44 bar. These conditions were maintained for 19 hours, then the vessel was cooled to 25 °C and depressurized before disassembly. The reaction mixture was decanted from the spent catalyst and rotary evaporated to recover the methanol-d_4 and to give a crude yellow liquid. The product was vacuum distilled (with assistance of a microcapillary) to recover 1-methyl-d_3-imidazole as a colorless liquid (9.01 g, 66.2%). GC/MS: *m/z* (EI) 88 (28.2), 87 (96.0), 86 (148.8), 85 (M^+, 100.0). NMR ($CDCl_3$) : δ_H 6.82 (H-4, s), 6.98 (H-5, s), 7.36 (H-2, s); δ_C 119.83 (C-5), 129.11, 128.96 (C-4, d), 137.56 (C-2), 32.39 (CD_3, septet, $^1J_{^{13}C-^2H} = 21$ Hz).

Deuterium exchange of 1-methyl-d_3-imidazole to give 1-methylimidazole-d_6

This exchange is derived from a combination of prior published methods.[27,28] Briefly, dry palladium catalyst (1 g Pd/C) was well stirred for 1 hr in a double-necked flask purged with nitrogen followed by capping one neck of the flask with a 230-mm round balloon full of hydrogen. A hose, connected to the second neck of the flask, allowed hydrogen to flow through the flask and through a water bath at a rate of ~1 bubble per second via a needle valve. 1-methyl-d_3-imidazole (5.03 g, 57.4 mmol) was dissolved in 25 g of D_2O, added to the reduced catalyst, degassed with three freeze-thaw cycles under slight vacuum, heated with stirring to 100 °C and held for 2 h. The product was filtered through a bed of celite and vacuum distilled to give 1-methyl-d_3-imidazole-*d* (4.25 g, 82%). In a sealed pressure tube, 1-methyl-d_3-imidazole-*d* (584 mg, 6.8 mmol) was dissolved in D_2O (20 g) and 63 mg of Pd/C was added. The tube was purged with hydrogen (as previously described), sealed, heated with stirring to 160 °C and held for 24 h. After cooling, the reaction mixture was diluted with H_2O (20 ml), filtered through a 0.2-μm nylon membrane, washed with H_2O (3×10 ml), and vacuum distilled to give 1-methylimidazole-d_6 (456 mg, 76%). GC/MS: *m/z* (EI) 89 (6.65) 88 (M^+, 100.0), 87 (29.9), 86 (17.6). NMR ($CDCl_3$) : δ_C/ppm 119.03, 119.50, 119.96 (C-5, triplet), 128.42, 128.88, 128.34 (C-4, triplet), 136.82, 137.32, 137.82 (C-2, triplet), 32.39 (CD_3, septet, $^1J_{^{13}C-^2H} = 21$ Hz).

GC/MS of imidazoles

All measurements were carried out with a Varian 4000 ion trap mass spectrometer (Walnut Creek, CA) coupled to a Varian 3800 gas chromatograph that was equipped with a CTC Analytics Combi-Pal autosampler (Zwingen, Switzerland). A Siltek-passivated single-gooseneck liner (Restek, Bellefonte, PA) and a RXi-1ms (30 mm long × 0.25 mm inner diameter, 0.25 μm film thickness, Restek, Bellefonte, PA) were used. Split (200 : 1) injections (1 μl) were performed. Operating conditions: injector temperature, 275 °C; carrier gas, helium at 1.0 ml/min; oven temperature program, 40–125 °C at 15 °C/min. The mass spectrometer was operated in positive electron ionization mode (70 eV) over a range of *m/z* 40–125 at the following temperatures: source, 170 °C; manifold, 40 °C; transfer line, 275 °C.

Plant cell wall preparation for NMR

Ball-milled wood was prepared from *Pinus taeda* sapwood, *Populus tremuloides* sapwood, and *Hibiscus cannabinus* bast fiber (1-year-old Tainung2 kenaf). Sequentially, 5 g of plant material was chopped into approximately 2 × 10 mm pieces, placed into a Retsch (Newtown, PA) MM 301 mixer mill (equipped with two 50-ml stainless steel jars, each with one 25-mm stainless steel ball bearing at −196 °C) for 2 min at 30 Hz. After the mixer mill, *Hibiscus cannabinus* was the only species Soxhlet extracted sequentially with water, 80% ethanol, and acetone to isolate the cell wall (essentially free of chlorophyll and other extractives). The wood species were not extracted for reasons we describe in the results and discussion. Then, 2 g of pulverized plant material was loaded into a Retsch PM 100 planetary ball-mill (equipped with a 50-ml ZrO_2 jar and ten 10-mm ZrO_2 ball bearings) and milled for 7 h (600 rpm, 10 min. pause every 20 min.); the jar temperature remained at <50 °C.

Plant cell wall dissolution

To a 5-ml flask, ball-milled plant cell wall material (60 mg) was added, followed by DMSO-d_6 (400 μl) and 1-methylimidazole-d_6 (100 μl) and stirred at room temperature to give a concentration of 120 mg/ml. A clear solution formed in approximately 3 h, depending on the sample, but was usually stirred overnight. Using a 178-mm NMR tube pipette, the viscous solution was transferred directly to a 5-mm NMR tube.

NMR, general

For imidazoles in $CDCl_3$, NMR spectra were acquired at 27 °C on a Bruker DRX-360 instrument (^1H 360.13 MHz, ^{13}C 90.56 MHz) fitted with a 5 mm ^1H/broadband gradient probe with inverse geometry (proton coils closest to the sample). Proton and carbon spectra were referenced to internal tetramethylsilane (TMS) at 0 ppm. For plant cell wall samples, NMR spectra were acquired at 27 °C on a Bruker DMX-500 (^1H 500.13 MHz, ^{13}C 125.76 MHz) instrument equipped with a sensitive cryogenically cooled 5-mm TXI $^1H/^{13}C/^{15}N$ gradient probe with inverse geometry. The central solvent peak was used as an internal reference for plant cell walls, DMSO (δ_C 39.5, δ_H 2.49 ppm). All processing and numerical integration calculations, utilizing single specimen data, were conducted using Bruker Biospin's TopSpin v. 2.0 software. Performing such integrations on NMR data from polymeric materials is sensitive to crosspeak overlap, thus all integrations were measured only on intense well-resolved crosspeaks.

Routine 1D ^1H and ^{13}C NMR spectra

^1H and ^{13}C spectra were recorded with 32K data points for a spectral width of 3094 Hz (8.6 ppm) and 64K data points for a spectral width of 20 000 Hz (220 ppm), respectively. Exponential multiplication (LB = 0.3 for ^1H, 2.0 for ^{13}C) and one level of zero-filling was performed prior to Fourier transformation.

2D HSQC spectra

The standard Bruker pulse implementation (invietgssi) of the gradient-selected sensitivity-improved inverse (^1H-detected) HSQC experiment[29] was used for acquiring the 2D spectra. The phase-sensitive HSQC spectra were determined with an acquisition time of 183 ms using an F_2 spectral width of 3501 Hz (7 ppm)

Copyright © 2008 John Wiley & Sons, Ltd.

in 1280 data points using 88 transients (16 dummy scans) for each of 400 t_1 increments of the $\boldsymbol{F_1}$ spectral width of 16 349 Hz (130 ppm) (F_1 'acquisition time' of 12.2 ms). Processing used a Gaussian function for $\boldsymbol{F_2}$ (LB = −0.18, GB = 0.005) and a cosine squared function for $\boldsymbol{F_1}$ prior to 2D Fourier transformation. The resulting data matrix was 1024 × 1024 points. ^{13}C-decoupling during acquisition was performed by GARP composite pulses from the high-power output decoupling channel.

NMR assignments

All polysaccharide ^{1}H and ^{13}C chemical shift assignments for the plant species described here were assigned using previous literature on *Populus tremula,*[30] *Linum usitatissimum,*[31] and *Picea abies*.[14,32,33] Lignin assignments were confirmed with the NMR database of lignin and cell wall model compounds.[34] Assignment of several polysaccharide crosspeaks were not attempted here, but research is underway toward further assignments.

Results and Discussion

Preparing the plant cell walls

The steps in preparing the plant material for dissolution are crucial for acquiring quality NMR spectra. The existing dissolution method[5] provided the basis for this program that involves decreasing the number of steps toward dissolution. The new method is designed to decrease material losses, eliminate the acetylation and subsequent isolation steps, decrease the sample preparation time, and be able to analyze milligram scale quantities. In particular, if an ethylenediamime tetraacetic acid (EDTA, chelating) wash step is deemed necessary to remove the paramagnetic iron from the material (to increase relaxation behavior for high-resolution spectra), ∼10% wt loss of cell wall material can result. Also, we wanted to eliminate the extraction steps, which remove low molecular weight compounds from the cell wall, but are also capable of disrupting the hydrogen bond network of polymeric components. The major reason for analyzing the cell wall in a nonextracted state is for the purposes of better understanding the reactivity of all plant components (including low molecular compounds in the cell lumina) toward derivatization, which is a project currently under investigation. Figure 1 illustrates the process we used for dissolving the plant cell walls, beginning with chopped plant material and ending with ball-milled micron-sized agglomerates for NMR analysis. Through environmental scanning electron microscope (ESEM) imaging of several samples, the mixer-milled material gave an estimated particle size of 100 μm and the ball-milled material was estimated to be <5 μm prior to dissolution.

Synthesis of NMI-d_6

The dissolution method requires synthesis of the perdeuterated 1-methylimidazole by *N*-methylation with deuterated methanol and exchanging the hydrogens at the 2, 4, and 5 positions on the ring with deuterium. The *N*-alkylation route we pursued was based on a ruthenium-trialkylphosphite complex to alkylate acidic NH groups of azoles.[26] A modification of this procedure uses methanol-d_4, which has been shown to give *N*-alkylation of imidazole in 49% yield.[27] Alkylation by this method in our lab gave an isolated yield of 66% (after vacuum distillation with a micro-capillary nitrogen bleed). GC/MS analysis of the product showed complete (−CD_3) *N*-methylation with a distribution of products with the ring protons exchanged, as well. For example, the expected 1-methyl-d_3-imidazole (27%) was found in addition to 1-methyl-d_3-imidazole-*d* (40%), 1-methyl-d_3-imidazole-d_2 (26%), and 1-methylimidazole-d_6 (7%).

After *N*-methylation, further exchange of the protons on 1-methyl-d_3-imidazole was accomplished. Imidazoles are much less prone to isotope exchange than their corresponding imidazolium salts.[35,36] Previous researchers used D_2O with the heterogeneous catalyst palladium (10%) on activated carbon to exchange all ring protons to give an yield of 91%.[27] In our several attempts with this method, the only position that exchanged to a high degree was H(2) with very little H(4/5) exchange. Since palladium catalysts seem to be quite variable in their activity with this method, our result prompted the search for a more consistent ring proton exchange method for H(4/5). Other researchers described a method of deuterium exchange of heterocyclic compounds with D_2O and heterogeneous Pd/C under 2.5 atm of hydrogen at 160 °C.[28] Although they did not study 1-methylimidazole, most heterocycles studied displayed almost quantitative deuterium incorporation of aromatic ring protons. Utilizing a somewhat modified procedure, we achieved quantitative exchange of the H(4/5) protons, but little H(2) exchange. Therefore, to obtain high deuterium exchange of 1-methylimidazole ring protons, we incorporated modifications of both procedures, to give an overall yield of ∼62% of the fully deuterated material. Figure 2 shows the ^{1}H spectra of the various stages in perdeuteration of 1-methylimidazole.

Plant cell wall dissolution

In the system previously described,[5] the DMSO : NMI ratio was 2 : 1 (v/v) with plant cell wall material at a concentration of 40 mg/ml. The solution becomes completely clear in a matter of 3 h or less, giving strong evidence of dissolution. For dissolution of plant cell walls to be directly placed into a 5-mm NMR tube, this would mean that only 20 mg of plant cell wall material would be dissolved in 0.5 ml. Particularly for 1D ^{13}C NMR, analyzing less than 60 mg of plant cell walls in 0.5 ml of solvent requires a very high number of scans (i.e. days rather than hours), especially if the cell wall component of interest is lignin, typically only ∼20% of the cell wall. We found that the use of DMSO-d_6 and NMI-d_6 in a ratio of 4 : 1 (v/v), to give a cell wall concentration of 120 mg/ml, was sufficient for dissolution. Clarity of the solution at this concentration is not as high, and the solution is also quite viscous; however, such solutions are still quite suitable for 2D NMR.[37] Spectra reacquired on identical samples after several months were identical and showed no degradation.

^{13}C/^{1}H NMR of the plant cell wall

The spectra described in the following figures contain color-coded contours, which correspond to their respective colored structure shown in Fig. 3. In Fig. 4, we show HSQC 1-bond ^{13}C–^{1}H correlation spectra for all the three species investigated: the gymnosperm *Pinus taeda* (loblolly pine), the angiosperm *Populus trembuloides* (quaking aspen), and the herbaceous plant *Hibiscus cannabinus* (kenaf). All the major cell wall components are depicted, including polysaccharides (aliphatic and anomeric regions) and lignin (side-chain and aromatic) regions. The enhanced peak dispersion and sensitivity using a cryogenically cooled sample probe allows for the potential to fully assign

Copyright © 2008 John Wiley & Sons, Ltd.

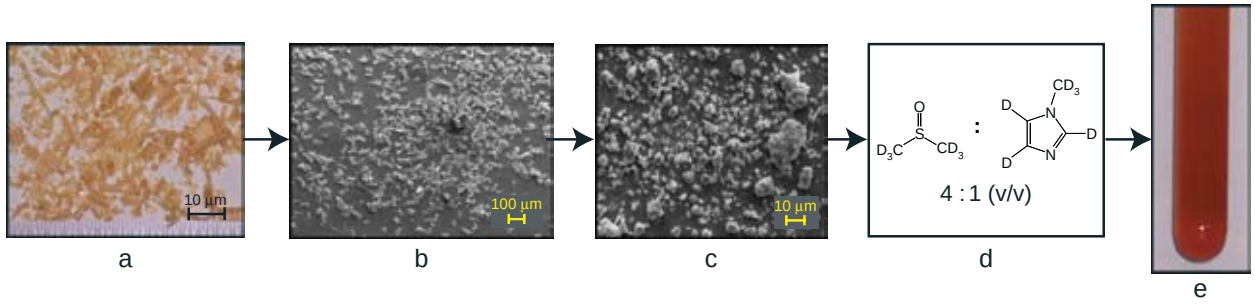

Figure 1. A diagram illustrating the nonderivatized dissolution of plant cell walls. *Pinus taeda* is shown here as an example: a, shavings produced via conventional planer; b, cryogenically mixer-milled; c, planetary ball-milled; d, dissolution method; e, NMR tube of cell walls in solution.

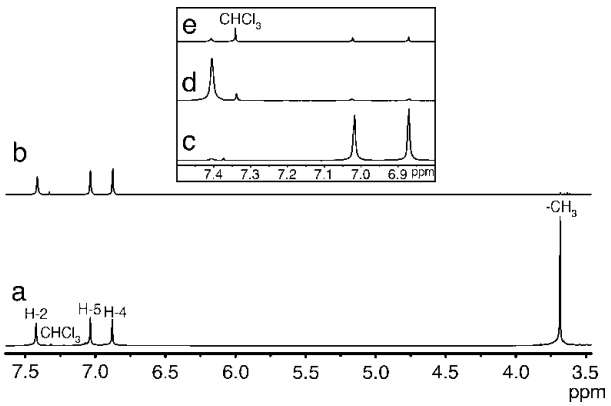

Figure 2. Proton spectra of various stages in NMI deuteration: a, 1-methylimidazole; b, 1-methyl-d_3-imidazole; c, ring deuteration as per Hardacre *et al.*[27]; d, ring deuteration as per Esaki *et al.*[28]; e, ring deuteration with combination of methods.

the polymeric structures in the whole cell wall. In the aromatic region, one of the major differences between angiosperms and gymnosperms is evident; angiosperms have both syringyl and guaiacyl units, while gymnosperms only have guaiacyl units. Angiosperm lignins are known to accommodate a higher β-aryl ether (A) content, a lower phenylcoumaran (B) content, and have an increased proportion of resinol (C) units compared to the gymnosperms. It is also quite noticeable that the kenaf has the lowest lignin content of the three, and consequently contains a proportionately larger quantity of polysaccharides, as seen by the intense anomeric correlations. It is evident that most of the polysaccharide anomeric correlations are fairly well resolved, allowing for partial characterization of the H-1/C-1 crosspeaks of glucan (cellulose), xylan, mannan, galactan, and arabinan. Here, we focus on assignments of lignin side-chain units, lignin guaiacyl and syringyl aromatics, naturally acetylated structures, and polysaccharide anomerics.

(i) Lignin side-chain units

Figure 5 shows the remarkably well-resolved lignin side-chain correlations for all the three species. Depicted are the major β-aryl ether units (A), phenylcoumaran units (B), resinol units (C), dibenzodioxocin units (D), cinnamyl alcohol endgroups (X1), and the lignin methoxyls (–OMe). The β-aryl ether units are well dispersed. For example, if a

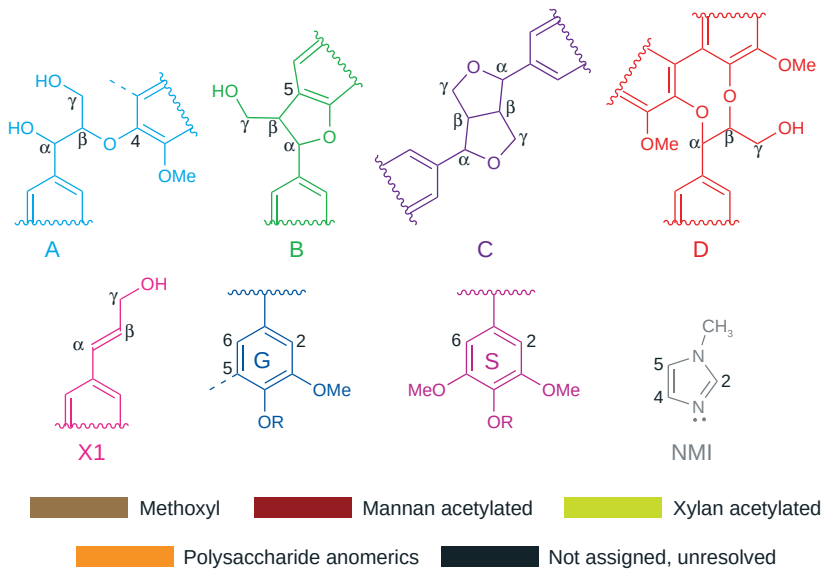

Figure 3. Key to the chemical structures found in the spectra in Figs 4–7. The structures are: (A) β-aryl ether in cyan, (B) phenylcoumaran in green, (C) resinol in purple, (D) dibenzodioxocin in red, (X1) cinnamyl alcohol endgroups in magenta, (G) guaiacyl in dark blue, (S) syringyl in fuchsia, and (NMI) 1-methylimidazole in gray. Other structures include: lignin methoxyl in brown, H-2/C-2 & H-3/C-3 correlations for the acetylated structure of β-D-Manp^I in maroon, H-2/C-2 & H-3/C-3 correlations for the acetylated structure of β-D-Xylp^I in chartreuse, polysaccharide anomerics in orange, and structures currently not assigned or unresolved in black.

Copyright © 2008 John Wiley & Sons, Ltd.

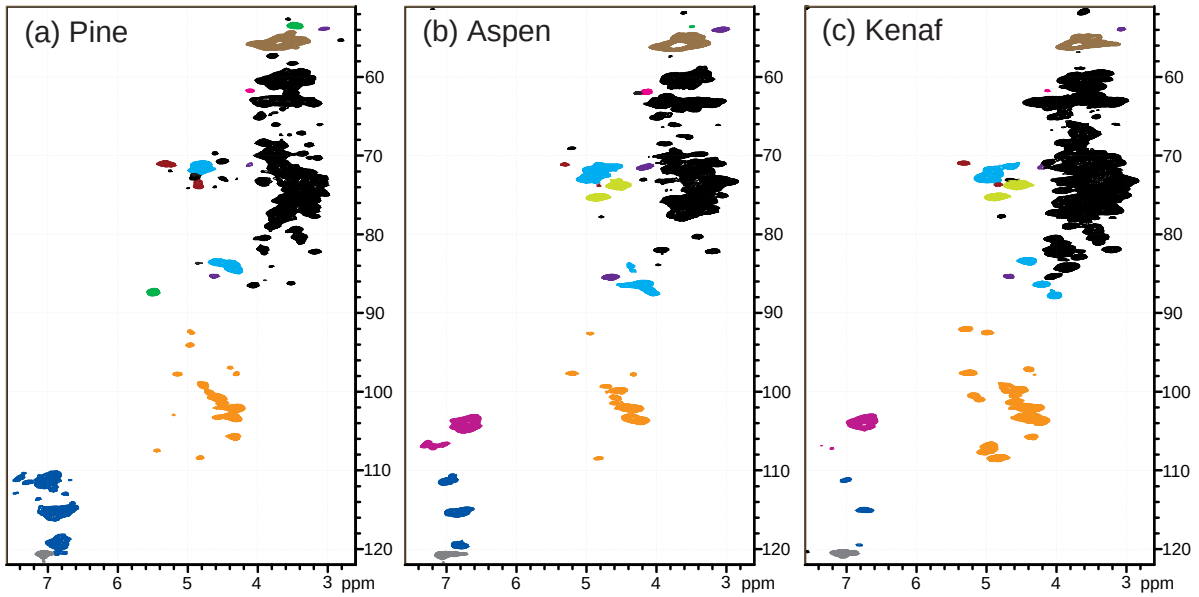

Figure 4. HSQC spectra from nonderivatized plant cell walls: a, pine; b, aspen; and c, kenaf at 500 MHz. Note that the spectra cover the range for all the cell wall components – cellulose, hemicelluloses, and lignin. All contour colors can be matched to their respective structures in Fig. 3. Expanded regions are shown in Figs 5–7.

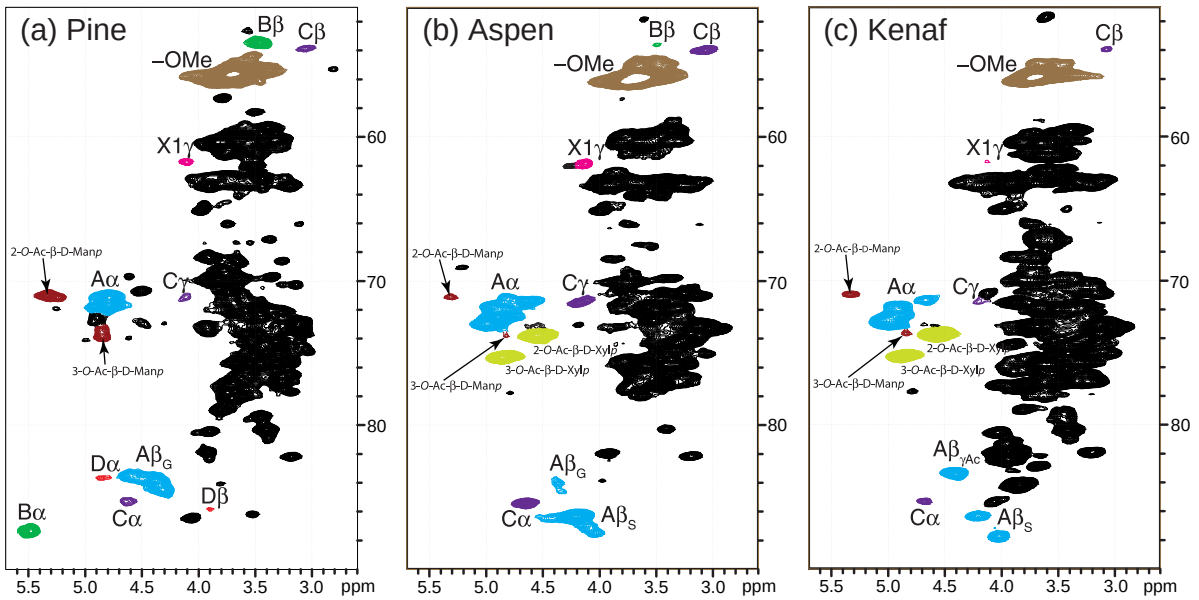

Figure 5. Aliphatic region of the whole plant cell wall HSQC spectra: a, pine; b, aspen; and c, kenaf. The black contours are currently unresolved, mostly because of heavy overlapping in these regions. All contour colors and labels can be matched to their respective structure in Fig. 3. As noted in the text, Aβ_G is any syringyl or guaiacyl coupled to a guaiacyl β-aryl ether, Aβ_S is any syringyl or guaiacyl coupled to a syringyl β-aryl ether, and A$\beta_{\gamma Ac}$ is a tentative assignment for a β-aryl ether linkage with a γ-acetate. 2-*O*-Ac-β-D-Man*p*, H-2/C-2 correlation for the acetylated structure of β-D-Man*p*^{I}; 3-*O*-Ac-β-D-Man*p*, H-3/C-3 correlation for the acetylated structure of β-D-Man*p*^{I}[32]; 2-*O*-Ac-β-D-Xyl*p*, H-2/C-2 correlation for the acetylated structure of β-D-Xyl*p*^{I}; 3-*O*-Ac-β-D-Xyl*p*, H-3/C-3 correlation for the acetylated structure of β-D-Xyl*p*^{I}[30,31].

guaiacyl or syringyl unit couples with a guaiacyl at the β-position of a β-aryl ether linkage (Aβ_G), the Aβ correlation is shown at 4.37/84.0 ppm.[34] This correlation clearly separates from the correlations where a guaiacyl or syringyl unit couples with a syringyl at the β-position (Aβ_S) shown at 4.19/86.3 ppm and 4.02/87.7 ppm.[34] The pine, having exclusively guaiacyl units, displays strong phenylcoumaran correlations (Bα, 5.48/87.4 ppm; Bβ, 3.46/53.5 ppm),[34] which are only visible in the aspen and kenaf at lower contour levels (not shown). Syringyl structures, with the additional methoxyl group at the 5 position on the ring, prevent the formation of linkages such as the phenylcoumaran and the 5–5-linked portion of dibenzodioxocins. Resinol correlations (Cα, 4.64/85.3 ppm; Cβ, 3.05/53.9 ppm; Cγ_1, 4.20/71.5 ppm)[34] are shown to be more significant in the aspen and kenaf than in pine. Generally, Cγ correlations are only visible in isolated milled-wood lignins; the Cγ_2 correlation remains masked by polysaccharides. The dibenzodioxocin correlations Dα and Dβ in pine are shown here to reside at 4.86/83.6 ppm and 3.90/85.8 ppm.[34] The cinnamyl alcohol endgroup

Copyright © 2008 John Wiley & Sons, Ltd.

correlation X1γ is shown at 4.14/61.7 ppm[34] and is visible in all the three species. Spirodienone/$\beta-1$ structures were detected in the aspen spectra only; however, because of the low quantity of such linkages in lignin (about 1.8% in aspen lignin),[38] the spectrum showed these only at low contour intensity. Spirodienone correlations Sα, Sβ, and Sβ' (not shown) were found at 5.14/81.4 ppm, 2.81/60.3 ppm, and 4.18/79.8 ppm.[38,39] Lignin methoxyls, typically a strong and broad contour, show some separation between the guaiacyl and syringyl methoxyls in the aspen and kenaf spectra.[34]

(ii) Lignin guaiacyl and syringyl aromatics

In Fig. 6, we show the lignin aromatic regions for the three species. Some interesting differences between the aspen and the kenaf spectra can be seen. In the aspen spectra, it is evident that the syringyl : guaiacyl ratio is much lower than with the kenaf; the pine thus showing exclusively guaiacyl units. With this dissolution method, since we are viewing the whole cell wall, we have the capability of estimating the syringyl : guaiacyl (S : G) ratio in the aromatic region of the lignin. Figure 6 shows the syringyl (S) and guaiacyl (G) correlations of the aromatic C–H groups in four basic conglomerates: S-2/6, G-2, G-5/6, and G-5. Previous literature suggested that the S : G ratio in kenaf and aspen lignin to be between 4.3–7.8 and 1.6–2.2, respectively.[40–42] Through volume integration of the S (S-2/6) and G (G-2, G-5/6, G-6) contours of the kenaf and aspen cell wall HSQC spectra, we determined the ratios to be 4.6 and 2.0, respectively, which falls into the expected ranges. The syringyl correlations shown are from β-aryl ether (A) and resinol (C) lignin units, while the guaiacyl correlations are from β-aryl ether (A), phenylcoumaran (B) and resinol (C) lignin units. The correlation at 7.07/120.5 ppm is from the residually protonated H-5/C-5 of 1-methylimidazole solvent, which, even though greatly suppressed, is still visible in the aromatic region.

(iii) Naturally acetylated structures

An interesting feature of kenaf lignin is its extensive acetylation of syringyl units with all the acetate on the γ-position of the β-aryl ether side chain. Thus, it appears that approximately two-thirds of the β-aryl ether units are acetylated.[23,43] The Aγ-acetate contours, undoubtedly present in the kenaf spectrum, are unfortunately found in a region highly overlapping with polysaccharide contours of the spectrum (4.15–4.45, 63.2 ppm), shown in Fig. 5. We cannot, using these spectra, assign any clear correlation to these acetylated Aγ's; however, the extended contour in this region suggests its existence. Logically, if the γ-OH is acetylated, an Aβ correlation around 4.62/84.6 ppm should be present (compound 3071, Ref. [34]). In the syringyl Aβ region for aspen and kenaf, there are two contours, 4.19/86.3 ppm and 4.02/87.7 ppm, as discussed previously. Aspen shows some guaiacyl Aβ correlation (4.37/84.0 ppm); however, in the kenaf spectrum a strong correlation exists in a similar region where a guaiacyl Aβ typically resides (4.41/83.4 ppm). As noted in Fig. 6, kenaf contains few guaiacyl units. Hence, this strong correlation is consistent with the Aβ on γ-acetylated β-aryl ether units, e.g. likely evidence of the Aγ acetate. Thus, the kenaf Aβ at 4.41/83.4 ppm has been tentatively labeled A$\beta_{\gamma Ac}$ in Fig. 5.

Another contour of interest for acetate quantification is the acetate methyl group. All the three species studied show a large contour centered at 1.99/20.9 ppm corresponding to the acetate methyls (see supplementary material). We integrated these acetate contour regions in all the spectra and compared them to those of the methoxyl correlations. The values obtained show that for pine, aspen, and kenaf, the ratio of methoxyl to acetate was 1 : 0.1, 1 : 0.3, and 1 : 0.6, respectively. Knowing that the syringyl (β-aryl ether type) units of kenaf are ~60% acetylated,[43] and that syringyl units predominate the lignin portion, an 1 : 0.6 ratio of methoxyl : acetate is a reasonable estimate and an indication that a large portion of the acetates are on lignins. Furthermore, a distinctive difference between the kenaf acetate contour compared to those in aspen and pine is an extended contour region at 1.75/20.3 ppm. Aspen syringyl units are only ~4% acetylated[43,44]; acetylated xylans may contribute largely to the acetate content. The major component of angiosperm hemicelluloses is an *O*-acetyl-4-*O*-methylglucurono-β-D-xylan (~16% of aspen and ~13% of kenaf cell wall),[45] where about 7 out of 10 xylose residues contain an *O*-acetyl group at C-2 or C-3.[46] The 2-acetylated xylan (2-*O*-Ac-β-D-Xyl*p*) and the 3-acetylated xylan (3-*O*-Ac-β-D-Xyl*p*) H-2/C-2 and H-3/C-3 correlations (shown in Fig. 5) are depicted at 4.56/73.8 ppm and 4.85/75.2 ppm, respectively, in aspen and kenaf.[30,31] The relative ratio of 3-*O*-Ac-β-D-Xyl*p*: 2-*O*-Ac-β-D-Xyl*p* was estimated from contour integration to be 1 : 1.12 in aspen and 1 : 1.29 in kenaf. Previous literature on an isolated 4-*O*-methylglucuronoxylan in aspen shows that the 2-*O*-acetylated xylose units are approximately one-third less abundant than the 3-*O*-acetylated xylose units.[30] However, *O*-acetyl migration during isolation methodologies makes this estimation difficult to ascertain.[47] For the pine, no data exists to support acetates on guaiacyl lignin. Thus, the acetates are expected to be on the mannans (~10% of loblolly pine hemicelluloses),[45] in particular galactoglucomannan, the principal hemicellulose component in gymnosperms. For the angiosperms, glucomannans are a secondary hemicellulose component, comprising ~2% of aspen and kenaf hemicelluloses.[45] The C-2 and C-3 positions of the mannan chain are partially substituted with *O*-acetyl groups in a frequency of about 1 out of 3–4 hexose units.[46] The acetylated mannan (2-*O*-Ac-β-D-Man*p* and 3-*O*-Ac-β-D-Man*p*) H-2/C-2 and H-3/C-3 correlations (shown in Fig. 5) are evidenced at 5.33/71.0 ppm and 4.85/73.8 ppm.[32,33] Previous researchers have shown that the ratio of 2-*O*-Ac-β-D-Man*p*: 3-*O*-Ac-β-D-Man*p* in Norway spruce is not equal, with the 2-*O*-Ac-β-D-Man*p* slightly predominating (e.g. 2.2 : 1, 1.7 : 1, and 1.1 : 1).[14,32,48] Here, through volume integration of the above contours, we report a ratio of 1.5 : 1 for loblolly pine.

(iv) Polysaccharide anomerics

In Fig. 7, we show the anomeric region for all the three species tentatively assigning several anomerics, including D-glucan, D-xylan, D-mannan, and D-galactan as the major contours. All the three spectra show internal anomerics of the (1→4)-linked β-D-glucopyranoside (β-D-Glc*p*^{I}) at 4.38/103.1 ppm,[31–33] as well as the (1→4)-linked β-D-xylopyranoside (β-D-Xyl*p*^{I}) at 4.32/102.1 ppm[30] and (1→4)-linked β-D-mannopyranoside (β-D-Man*p*^{I}) at 4.57/100.7 ppm.[32,33] The pine depicts anomeric correlations of the terminal α-D-galactopyranoside (α-D-Gal*p*^{T}), (1→6)-linked to β-D-Man*p*, at 4.84/99.0 ppm.[32,33] The pine and kenaf spectra also show anomeric correlations of a terminal β-D-galactopyranoside (β-D-Gal*p*^{T}), (1→6)-linked to β-D-Man*p*,

Copyright © 2008 John Wiley & Sons, Ltd.

Magnetic Resonance in Chemistry

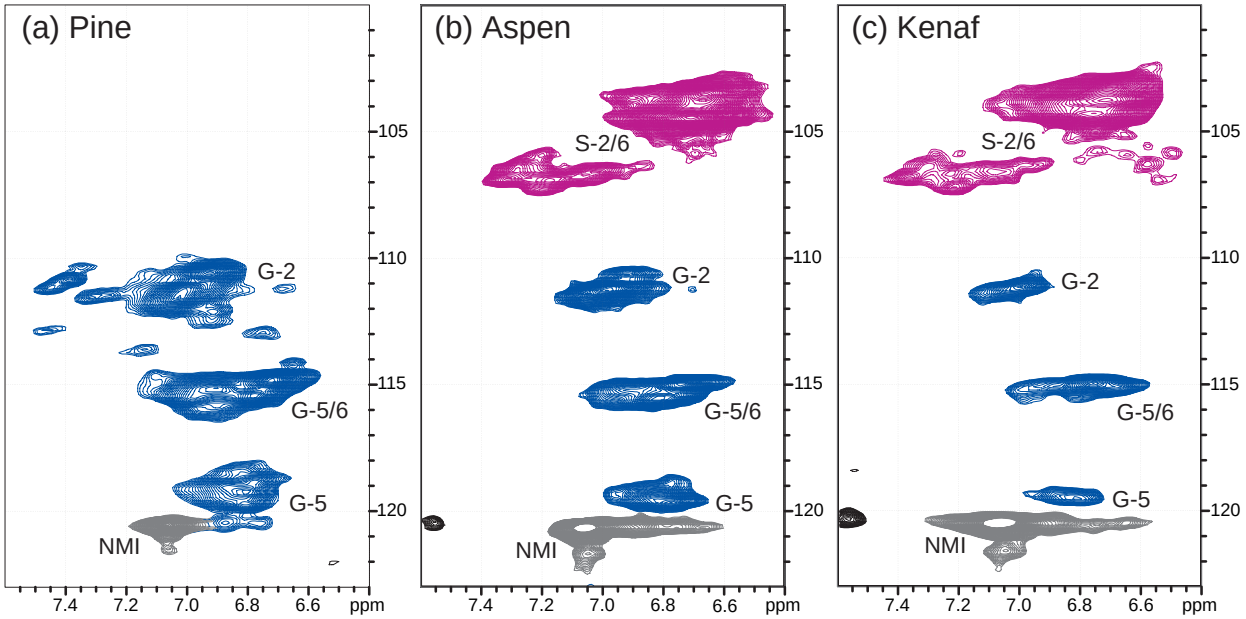

Figure 6. Aromatic region of the whole plant cell wall HSQC spectra: a, pine; b, aspen; and c, kenaf. The guaiacyl and syringyl contours are a combination of free phenolic and etherified aromatic units. Contour colors and labels can be matched to their respective structure in Fig. 3.

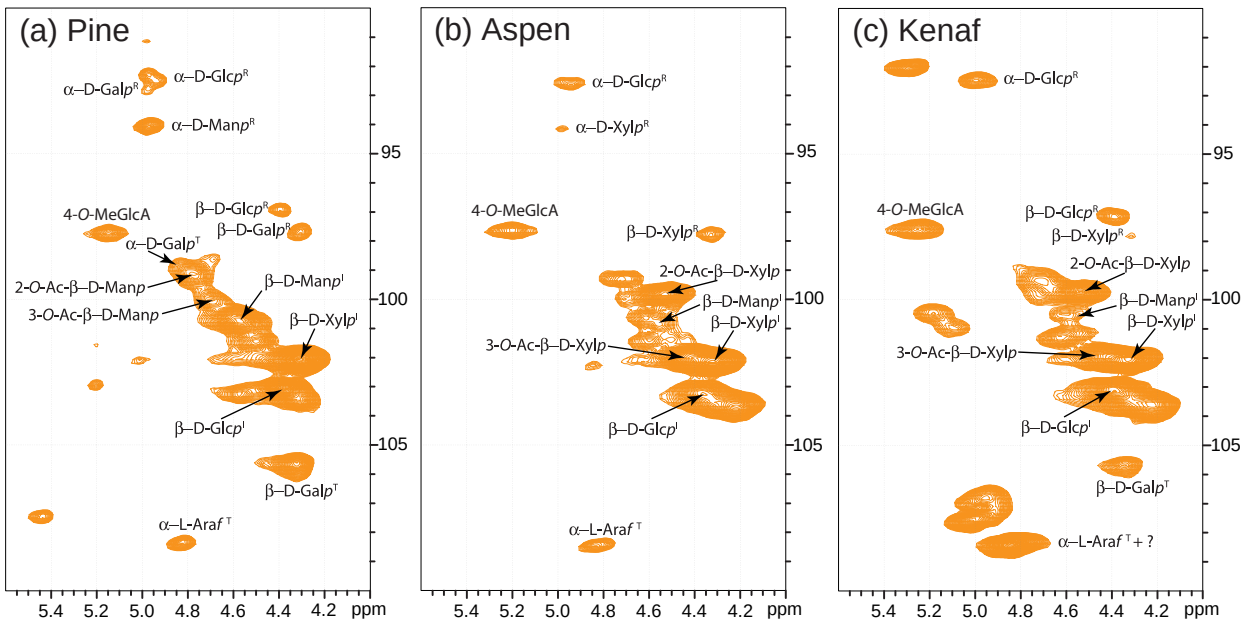

Figure 7. Anomeric region of the whole plant cell wall HSQC spectra: a, pine; b, aspen; and c, kenaf. Assignments are as follows: β-D-Glc*p*^{I}, internal β-D-glucopyranoside units (cellulose)[31–33]; β-D-Man*p*^{I}, internal β-D-mannopyranoside units[32,33]; β-D-Xyl*p*^{I}, internal β-D-xylopyranoside units[30]; α-D-Gal*p*^{T}, terminal α-D-galactopyranoside units[32,33]; β-D-Gal*p*^{T}, terminal β-D-galactopyranoside units[33]; α-L-Araf^{T}, terminal α-L-arabinofuranoside units[31,32,50]; 2-*O*-Ac-β-D-Man*p*, anomeric correlation for the acetylated H-2/C-2 structure of β-D-Man*p*^{I}; 3-*O*-Ac-β-D-Man*p*, anomeric correlation for the acetylated H-3/C-3 structure of β-D-Man*p*^{I}[32]; 2-*O*-Ac-β-D-Xyl*p*, anomeric correlation for the acetylated H-2/C-2 structure of β-D-Xyl*p*^{I}; 3-*O*-Ac-β-D-Xyl*p*, anomeric correlation for the acetylated H-3/C-3 structure of β-D-Xyl*p*^{I}[30,31]; 4-*O*-MeGlcA, 4-*O*-methyl-α-D-glucuronic acid[30]; α and β-D-Glc*p*^{R}, reducing ends of glucopyranoside[32,33]; β-D-Man*p*^{R}, reducing end of mannopyranoside[32]; α and β-D-Gal*p*^{R}, reducing ends of galactopyranoside[33]; α and β-D-Xyl*p*^{R}, reducing ends of xylopyranoside.[30].

at 4.32/105.7 ppm,[32,33] which is absent in aspen. Acetylated mannan structures show their respective anomeric correlations at 4.78/99.1 ppm (2-*O*-Ac-β-D-Man*p*) and 4.69/100.0 ppm (3-*O*-Ac-β-D-Man*p*),[32] while the acetylated xylan structures show their respective anomeric correlations at 4.53/99.8 ppm (2-*O*-Ac-β-D-Xyl*p*) and 4.44/102.0 ppm (3-*O*-Ac-β-D-Xyl*p*).[30,31] Arabinoglucuronoxylan, 5–10% of the cell wall weight in gymnosperms, is a framework of (1→4)-linked β-D-Xyl*p*^{I} units that are substituted at C-2 by 4-*O*-methyl-α-D-glucuronic acid (4-*O*-MeGlcA) groups in a frequency of two residues per ten β-D-Xyl*p*^{I} units.[46] The 4-*O*-MeGlcA anomeric correlations for pine are depicted at 5.15/97.8 ppm. However, the 4-*O*-MeGlcA in the aspen and kenaf, (1→2)-linked in glucuronoxylan, depict their anomeric correlations

 Copyright © 2008 John Wiley & Sons, Ltd.

at 5.20/97.7 ppm and 5.25/97.7 ppm.[30] This variation in δ_H may be caused by the presence of the carboxylic acid; chemical shift changes in the DMSO-d_6/NMI-d_6 solvents would be expected. The arabinoglucuronoxylan is also substituted with terminal (1→3)-linked α-L-arabinofuranoside (α-L-Araf^T) units in a frequency of 1.3 residues per ten β-D-Xylp^I units.[46] The galactans of angiosperms are known to contain rhamnose and arabinose units, e.g. giving a molar ratio of 1.7 : 1 : 0.2 (Gal : Ara : Rha) in sugar maple.[49] Thus, the α-L-Ara*f* anomeric correlations for pine, aspen, and kenaf are depicted at 4.83/108.4 ppm.[31,32,50] Reducing ends of the polysaccharides can also be seen in the spectra and are tentatively assigned here. The reducing α and β ends of D-Glc*p* residues are shown at 4.94/92.7 ppm and 4.40/96.9 ppm.[32,33] For pine, the reducing α end of D-Man*p* and the reducing α and β ends of D-Gal*p* residues are shown at 4.97/94.0 ppm,[32,33] 4.98/92.8 ppm and 4.31/97.7 ppm.[33] For aspen, the reducing α and β ends of D-Xyl*p* residues are shown at 4.98/94.2 ppm and 4.33/97.8 ppm.[30] In the kenaf spectrum, only the reducing β end of D-Xyl*p* is observed.

Conclusions

The methodologies developed here help in characterizing the structures of several native-state plant cell wall components. Through the effective synthesis of perdeuterated 1-methylimidazole to a high degree of deuterium incorporation, we described an approach to dissolve ball-milled wood and characterize the majority of the plant cell wall components via high-resolution solution-state NMR. To directly dissolve ball-milled cell wall material in nondegradative solvents and run NMR of these samples allows characterization without derivatization. The HSQC 1-bond $^{13}C-^{1}H$ correlation spectra of pine, aspen, and kenaf depict all major plant cell wall components with excellent resolution, dispersion, and in their near-native state. Through these spectra, we assigned correlations to naturally acetylated mannan and xylan structures found in galactoglucomannan, glucomannan, and glucuronoxylan. The existence of a β-aryl ether γ-acetate, believed to exist in kenaf lignin, has been explored further through the tentative assignment of A$\beta_{\gamma Ac}$. The well-dispersed contours in the polysaccharide anomeric region of the HSQC spectra allowed us to tentatively assign several correlations in hemicelluloses. Through contour integration techniques, we estimated the ratios of cell wall structures. For example, literature values for the S : G ratio and acetate content match our data fairly closely. We assume that utilizing adiabatic sequences to remove *J*-dependence, and possibly applying determined response factors, will allow more accurate quantification in the future. More research needs to be done to define polysaccharide chemical shifts; most chemical shift data obtained for assignments were derived from oligosaccharides dissolved in D_2O, and not in DMSO-d_6/NMI-d_6. However, this research broadens the utility of the DMSO/NMI method to better understand plant cell wall chemistry, which may be applied to various fields. We are currently employing these methods to investigate chemical modification, microbiological decay mechanisms, and genetically engineered plants and trees.

Supplementary material

Supplementary electronic material for this paper is available in Wiley InterScience at http://www.interscience.wiley.com/jpages/0749-1581/suppmat/

Acknowledgements

We would like to thank especially Dr. Fachuang Lu, Dr. Hoon Kim, Dr. Takuya Akiyama, and Dr. Paul Schatz (U.S. Dairy Forage Research Center, Madison, WI) for assistance in establishing methodology and for very beneficial discussions on lignin chemistry and plant cell wall dissolution. Also, we would like to thank Kolby Hirth (USDA Forest Products Laboratory, Madison, WI) for GC/MS data analyses of the imidazoles. Partial funding to J.R. through the Office of Science (BER), U.S. Department of Energy, Interagency agreement No. DE-AI02-06ER64299 is gratefully acknowledged. NMR experiments on the Bruker DMX-500 cryoprobe system were carried out at the National Magnetic Resonance Facility at Madison, WI, which is supported by National Institutes of Health grants P41RR02301 (Biomedical Research Technology Program, National Center for Research Resources) and P41GM66326 (National Institute of General Medical Sciences). Additional equipment was purchased with funds from the University of Wisconsin, the National Institutes of Health (RR02781, RR08438), the National Science Foundation (DMB-8415048, OIA-9977486, BIR-9214394), and the U.S. Department of Agriculture.

References

[1] Barron PF, Frost RL, Doimo L, Kennedy MJ. *J. Macromol. Sci.-Chem.* 1985; **A22**: 303.
[2] Sterk H, Sattler W, Esterbauer H. *Carbohydr. Res.* 1987; **164**: 85.
[3] Bardet M, Emsley L, Vincendon M. *Solid State Nucl. Magn. Reson.* 1997; **8**: 25.
[4] Johnson CE, Smernik RJ, Siccama TG, Kiemle DK, Xu Z, Vogt DJ. *Can. J. For. Res.* 2005; **35**: 1821.
[5] Lu F, Ralph J. *Plant J.* 2003; **35**: 535.
[6] Björkman A. *Sven. Papperstidn.* 1956; **59**: 477.
[7] Chang H-M, Cowling EB, Brown W. *Holzforschung* 1975; **29**: 153.
[8] Ritter GJ, Kurth EF. *Ind. Eng. Chem.* 1933; **25**: 1250.
[9] Jayme G. *Cellul. Chem.* 1942; **20**: 43.
[10] Wise LE. *Ind. Eng. Chem., Anal. Ed.* 1945; **17**: 63.
[11] Klauditz W. *Holzforschung* 1957; **11**: 110.
[12] Sun RC, Tomkinson J. *Int. J. Polym. Anal. Charact.* 1999; **5**: 181.
[13] Sundberg A, Holmbom B, Willför S, Pranovich A. *Nord. Pulp Pap. Res. J.* 2000; **15**: 46.
[14] Capek P, Alföldi J, Lišková D. *Carbohydr. Res.* 2002; **337**: 1033.
[15] Fengel D, Stoll M, Wegener G. *Wood Sci. Technol.* 1978; **12**: 141.
[16] Maurer A, Fengel D. *Holzforschung* 1992; **46**: 417.
[17] Swatloski RP, Spear SK, Holbrey JD, Rogers RD. *J. Am. Chem. Soc.* 2002; **124**: 4974.
[18] Wu J, Zhang J, Zhang H, He J, Ren Q, Guo M. *Biomacromolecules* 2004; **5**: 266.
[19] Fort DA, Remsing RC, Swatloski RP, Moyna P, Moyna G, Rogers RD. *Green Chem.* 2007; **9**: 63.
[20] Pu Y, Jiang N, Ragauskas A. *J. Wood Chem. Technol.* 2007; **27**: 23.
[21] Xie H, King A, Kilpelainen I, Granstrom M, Argyropoulos DS. *Biomacromolecules* 2007; **8**: 3740.
[22] Heinze T, Dicke R, Koschella A, Kull AH, Klohr E-A, Koch W. *Macromol. Chem. Phys.* 2000; **201**: 627.
[23] Ralph J. *J. Nat. Prod.* 1996; **59**: 341.
[24] del Rio JC, Gutierrez A, Martinez AT. *Rapid Commun. Mass Spectrom.* 2004; **18**: 1181.
[25] del Rio JC, Marques G, Rencoret J, Martinez AT, Gutierrez A. *J. Agric. Food Chem.* 2007; **55**: 5461.
[26] Tanaka N, Hatanaka M, Watanabe Y. *Chem. Lett.* 1992; **21**: 575.
[27] Hardacre C, McMath SEJ, Holbrey JD. *Chem. Commun.* 2001; 367.
[28] Esaki H, Ito N, Sakai S, Maegawa T, Monguchi Y, Sajiki H. *Tetrahedron* 2006; **62**: 10954.
[29] Willker W, Leibfritz D, Kerssebaum R, Bermel W. *Magn. Reson. Chem.* 1992; **31**: 287.
[30] Teleman A, Lundqvist J, Tjerneld F, Stalbrand H, Dahlman O. *Carbohydr. Res.* 2000; **329**: 807.
[31] van Hazendonk MJ, Reinerink EJM, de Waard P, van Dam JEG. *Carbohydr. Res.* 1996; **291**: 141.

Copyright © 2008 John Wiley & Sons, Ltd.

[32] Hannuksela T, du Penhoat CH. *Carbohydr. Res.* 2004; **339**: 301.
[33] Capek P, Kubachova M, Alfoldi J, Bilisics L, Liskova D, Kakoniova D. *Carbohydr. Res.* 2000; **329**: 635.
[34] Ralph SA, Ralph J, Landucci L. NMR database of lignin and cell wall model compounds. 2004; http://www.dfrc.ars.usda.gov/software.html.
[35] Clement O, Roszak AW, Buncel E. *J. Am. Chem. Soc.* 1996; **118**: 612.
[36] Wong JL, Keck J Jr. *J. Org. Chem.* 1974; **39**: 2398.
[37] Kim H, Ralph J, Akiyama T. *Bioenergy Res.* 2007; in press.
[38] Zhang LM, Gellerstedt G. *Chem. Commun.* 2001; (4): 2744.
[39] Zhang L, Gellerstedt G, Ralph J, Lu F. *J. Wood Chem. Technol.* 2006; **26**: 65.
[40] Ralph J, Hatfield RD, Lu F, Grabber JH, Jung HG, Han JS, Ralph SA. *Proceedings of the 8th International Symposium on Wood and Pulping Chemistry*, Helsinki, Finland. Gummerus Kirjapaino Oy: Jyväskylä, Finland, 1995; 125.
[41] Lu F, Ralph J. *J. Agric. Food Chem.* 1998; **46**: 547.
[42] Li L, Zhou YH, Cheng XF, Sun JY, Marita JM, Ralph J, Chiang VL. *Proc. Natl. Acad. Sci. U.S.A.* 2003; **100**: 4939.
[43] Ralph J, Lu F. *J. Agric. Food Chem.* 1998; **46**: 4616.
[44] Timell TE. *Sven. Papperstidn.* 1969; **72**: 173.
[45] Davis MW. *J. Wood Chem. Technol.* 1998; **18**: 235.
[46] Sjöström E. *Wood Chemistry: Fundamentals and Applications* (2nd edn). Academic Press: San Diego, 1993.
[47] Reicher F, Corrêa JBC, Gorin PAJ. *Carbohydr. Res.* 1984; **135**: 129.
[48] Willför S, Sjöholm R, Laine C, Roslund M, Hemming J, Holmbom B. *Carbohydr. Polym.* 2003; **52**: 175.
[49] Fengel D, Wegener G. *Wood: Chemistry, Ultrastructure, Reactions*. Walter de Gruyter & Company: Berlin, 1983.
[50] Dourado F, Cardoso SM, Silva AMS, Gama FM, Coimbra MA. *Carbohydr. Polym.* 2006; **66**: 27.

 Copyright © 2008 John Wiley & Sons, Ltd.